Structural Eng./Earthquake Eng. Vol. 11, No. 2, 93s—101s, July 1994
Japan Society of Civil Engineers (J. Struct. Mech. Earthquake Eng. No. 495/ I—28)

DEPENDENCE ON FREQUENCY OF DYNAMIC INTER-PARTICLE DISLOCATION WITHIN A SLOPE

Kazuo KONAGAI*, Takashi MATSUSHIMA**
and Takeshi SATO***

Irreversible deformation of a coarse particle assemblage is mainly due to a change in its fabric, and this process is attended by a noticeable dilation which is confirmed through the new visualization technique (Laser-Aided Tomography: LAT). Numerical analysis by means of discrete elliptic element method (DEEM) is conducted to study the dilating process. The effect of both inter-particle slipping and rolling of embedded grains is discussed, and a simple conceptual model of slope failure, in which dilation leads to frequency dependence of the failure acceleration, is presented.

Key Words *: visualization, granular structure, frequency dependence.*

1. INTRODUCTION

In studying the earthquake resistance of such granular structures as rockfill dams, artificial islands made of sand and gravel, masonry foundations of off-shore and near-shore structures and so on, it is of the essence to study the dynamic changes in the fabric of an assemblage of coarse particles. Since natural materials including gravel and rocks are not easily tested in laboratory conditions, a model experiment is a useful tool providing us with important information on their failure process. The authors have developed, for this purpose, a new visualization technique, Laser-Aided Tomography [1),2)], which enables the observation of individual grain's behavior in the interior of a coarse particle assemblage. Using this method, Konagai, Tamura et al.[1),2)] and Hirata[3)] studied the dynamic response of an embankment model made up of coarse particles. The embankment model was shaken sinusoidally on a shaking table with the amplitude of base acceleration being increased with time. The particles near the surface began to move when the amplitude of acceleration exceeded a threshold. Differing from the phenomena governed by the Coulomb's hypothesis, the threshold increased with increasing excitement frequency, and the bigger the representative grain size was, the clearer the tendency was. This result is consistent with the findings by Tamura et al[4)] through their experiments on models of fill dams. Since this phenomenon is unique for coarse granular materials and differs from that observed in a finer grain assemblage, it should be taken into account when the dynamic stability of this kind of granular structures is discussed.

Discrete element method (DEM) is a powerful tool for studying the mechanism of this phenomenon because it provides quantitative information about the motion of all elements. In the DEM simulations presented in this paper, elliptic elements were used in order to take into account the effect of particles' shape on the behavior of a granular assemblage[5)]. Even though an actual grain is nothing like a complete ellipse, the study of oval elements' interaction will give us a general idea of the dilating process of a particle assemblage. Two embankment models made up of elliptic and circular disks, respectively, were shaken in the same manner. The differences in their failure processes were discussed examining the overall contributions to the failure of the two key motions of a grain, i. e., slip and roll. Finally, this paper presents a conceptual model of surface slide and shows that frequency dependence of failure acceleration is mostly due to a considerable volumetric increase, that is, dilation.

2. PROCESS OF FAILURE OBSERVED IN THE LAT EXPERIMENT

A new visualization technique called "Laser-Aided Tomography" (LAT), was developed for the study of the dynamic behavior of underwater granular structures[1),2)]. In this method, a granular structure model made of particles of crushed glass immersed in a liquid with the same refractive index becomes invisible.

* Member of JSCE, Dr. Eng., Associate Professor, Institute of Industrial Science, Univ. of Tokyo, (7-22-1, Roppongi, Minato-ku, Tokyo 106, JAPAN).
** Member of JSCE, M. Eng., Research Associate, Tokyo Institute of Technology, (2-12-1, Ookayama, Meguro-ku, Tokyo 152, JAPAN).
***Member of JSCE, M. Eng., NKK Corporation, (1-1-2, Marunouchi, Chiyoda-ku, Tokyo 100, JAPAN).

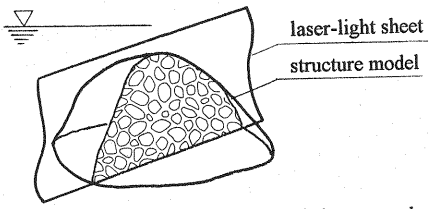

Fig. 1 Laser-aided tomography: LAT

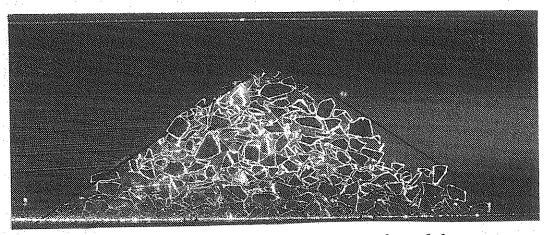

Fig. 2 Cross-section of rock-mound model

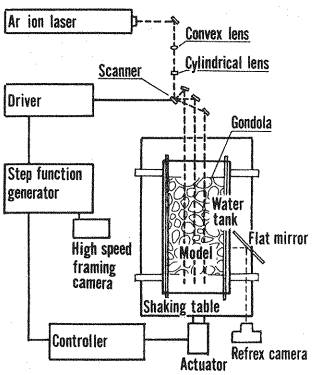

Fig. 3 Apparatus for LAT experiment

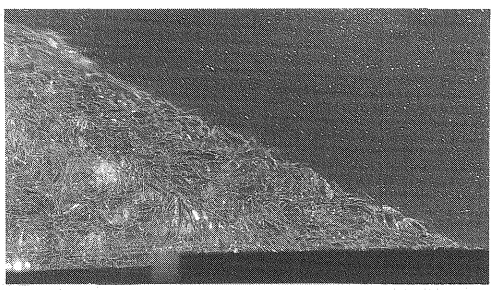

(a) t=5s, acceleration=20gal

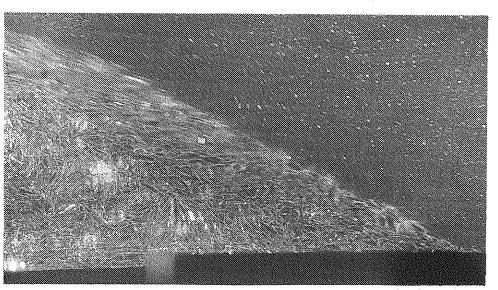

(b) t=7s, acceleration=28gal

Fig. 4 Cross-section of embankment model

An intense laser-light sheet (LLS) is then passed through the model illuminating the contours of all the particles on a cross-section optically cut by the LLS. Thus, scanning the model with LLS enables us to observe its whole-field deformation (**Figs. 1** and **2**).

Dynamic failure tests of embankment-shaped models were conducted using LAT. Coarse glass grains of two different sizes: fine (2 mm < grain < 5 mm) and medium (5 mm < grain < 12 mm) were piled up, within a gondola, into two embankment models with the same isosceles shape (height = 90 mm, slope = 1:2.72). The gondola was shaken sinusoidally within a water-tank full of liquid with the same refractive index as the glass (**Fig. 3**). The front and rear of the gondola were glazed, while both sides were open, and consequently, its motion did not stir the liquid much. A laser-light-sheet (LLS) traveled through the middle of the embankment's thickness. The amplitude of oscillation was increased linearly with time (4 gal/s). The embankment's surface began to slide when the base acceleration exceeded a threshold. Both **Figs. 4(a)** and **4(b)** show the cross-section of the embankment model made up of smaller grains (2 mm < grain < 5 mm). These photographs were taken at (a) and (b) in **Fig. 5**, respectively. **Fig. 5** shows variation with base acceleration of the cross-sectional area of the embankment. Obviously, the surface failure of the embankment is accompanied by a considerable dilation.

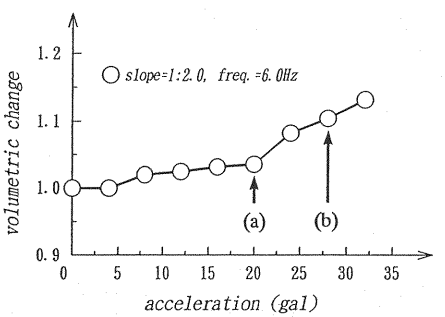

Fig. 5 Volumetric change ($V_{dynamic}$ / V_{static}) of embankment model

3. DISCRETE ELLIPTIC ELEMENT METHOD

Quantified values representing the motion of all grains making up a structure enable us to take a statistical approach to the understanding of the failure mechanism. In this sense, numerical simulations by means of discrete element method (DEM) are very useful, though the limited capacity and power of a computer at this stage still make it difficult to simulate the motions of as many particles as those actually piled in the LAT experiment. The DEM, originally developed by Cundall[6], treats granular material as an assemblage of distinct particles, each governed by physical lows. Each particle interacts with its neighbours through particle-to-particle contacts which are formed or broken at each time step. Once a contact is formed, the interaction force is represented by the normal and tangential forces induced in virtual contact springs. The equation of motion for each element is solved by step-by-step numerical integration in the time domain.

As confirmed through the performed LAT experiments, the motion of an irregularly-shaped particle confined within a coarse particle assemblage will be attended with a noticeable dilation of the assemblage. In order to take into account the effect of irregular grain shape on the dilating process, elliptic elements were used in the DEM calculations presented here. It goes without saying that the actual grain shape is not a complete ellipse. However, a study on oval particles' interaction will give us a general idea of the dilating process. This approach also has the advantage of saving calculation time because the check for a contact between two elements can be made not by numerical technique but by solving a 4th-degree equation analytically using Ferrari's method. The parameters used in this study are summarized in **Table 1**. A relatively high value of friction coefficient was set in order to take into account the angularity of real particles. Considering that deformation of an individual particle has less effect on overall behavior than inter-particle dislocation does, contact spring constants were set at relatively low values in order to save calculation time.

A change in the fabric of granular assemblage is related with inter-particle slipping and grain's rolling. These two key motions will have different effect on the overall failure of the assemblage. To study the effect of these two motions in a simple manner, an increasing sinusoidal shake was given to a slope with an ellipse on it. The aspect ratio of the ellipse (the ratio of minor axis to major one) and the gradient of the slope were 2 : 3 and 3 : 10, respectively. No sooner was a shake given to the slope, than the ellipse began to rock, and the amplitude of rocking increased gradually. When the amplitude of base acceleration exceeded a threshold, the ellipse began to roll down the slope in the case of lower frequency excitation (2 Hz, 4 Hz, 6 Hz), while it slipped down in case of higher frequency excitation (8 Hz, 10 Hz) (**Fig. 6**). **Fig. 7** shows the progressive displacement of this ellipse with increasing amplitude of base acceleration. Since the acceleration amplitude was linearly increased with time, the curves in this figure are regarded as time histories of the ellipse's

Table 1 Parameters for the DEEM simulation

Time increment	1.0×10^{-4} s
Density of element	2.0×10^{1} kg/m^2
Spring constant (normal)	3.0×10^{4} N/m
Spring constant (shear)	1.0×10^{4} N/m
Damping coefficient (normal)	5.0 kg/s
Damping coefficient (shear)	5.0 kg/s
Friction coefficient	1.0

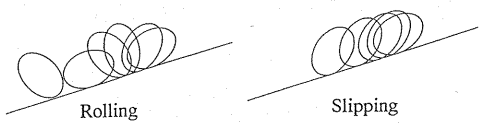

Fig. 6 Ellipse on shaking slope

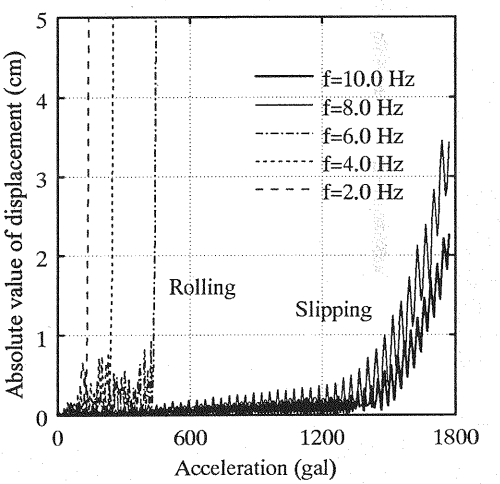

Fig. 7 Absolute value of displacement of an ellipse on shaking slope

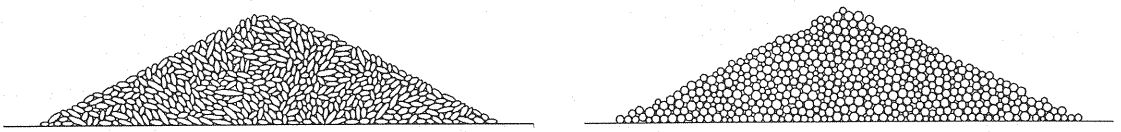

(a) 500 ellipses (**model A**)　　(b) 500 circles (**model B**)

Fig. 8 Piles of grains

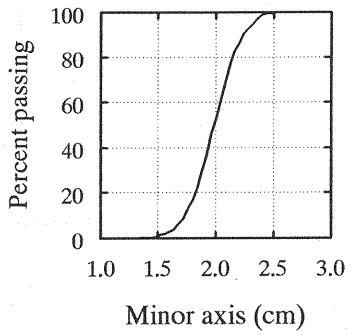

Fig. 9 Distribution curve of minor axis (**model A**)

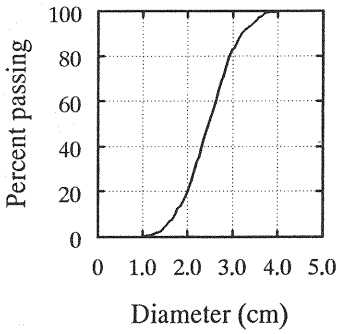

Fig. 10 Distribution curve of diameter (**model B**)

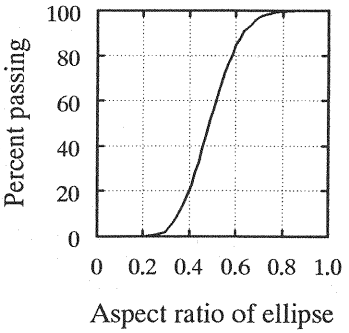

Fig. 11 Distribution curve of aspect ratio (**model A**)

displacement. When the ellipse began to roll down, clear frequency dependence of the threshold acceleration appeared, because its rocking or rolling leads to change in potential energy. On the contrary, when the ellipse slipped down, less dependence of the threshold appeared. This seems natural because the slipping threshold should depend only on the slope gradient and on the friction coefficient between the particle and the slope in contact. The displacement of a rolling ellipse progresses more rapidly than that of a slipping one.

500 ellipses and 500 circles were then piled up into two embankments (height and slope are about 25 cm and 1 : 2, respectively). **Figs. 8(a)** and **8(b)** show the piles of 500 ellipses (**model A**) and 500 circles (**model B**), respectively. The distributions of minor disk axes of the ellipses and diameters of the circles are shown in **Figs. 9** and **10**, respectively. The distribution of aspect ratios of the ellipses making up **model A** is shown in **Fig. 11**. The bottom particles of both models were bonded to the bases. An increasing sinusoidal shake (197 gal/s) was given to both their bases. **Fig. 12(a)** shows the whole-field pictures of the failure on the right-hand side of **model A**, and the displacements of the centers of all the elements are shown in **Fig. 12 (b)**. The elements near the slope surface moved down, while those interlocking in the depth of the model scarcely moved. The dilation, as a whole, progressed slowly and steadily as shown in **Fig. 13**, and no sudden volumetric increase was clearly seen. Thus, it was not possible in this simulation to specify a threshold acceleration. In both cases, however, the lower the excitement frequency is, the more rapidly the failure progresses, and this phenomenon is consistent with the result from the LAT experiments.

As has been mentioned before, a change in the fabric of granular assemblage is attended by both inter-particle slipping and grain rolling. Contributions of these two key motions to the failure process must be statistically studied in order to discuss the frequency dependence of the failure acceleration. For this purpose, overall displacement U_{ov} and overall rotation angle Φ_{ov} are defined here as:

$$U_{ov} = \sum_{j=1}^{n} |u_j| \qquad \Phi_{ov} = \sum_{j=1}^{n} |\phi_j| \qquad \cdots\cdots(1)$$

where, n= number of particles, u_j= displacement of j-th element and ϕ_j= rotation of j-th element. **Fig. 14** shows relation between the overall displacement U_{ov} and overall rotation angle Φ_{ov}. The contribution of inter-particle rolling is bigger in **model B** than in **model A**. It is noted that the contribution of inter-particle rolling to the failure process differs little in different excitement frequency in either case of **models A** and **B**. This implies that, given a specific grain assemblage, the rolling-slipping ratio within the grain fabric during its failure process will be uniquely determined. The thick dashed-and-dotted line shows the case of a particle with a typical size for these models rolling down a slope without slipping.

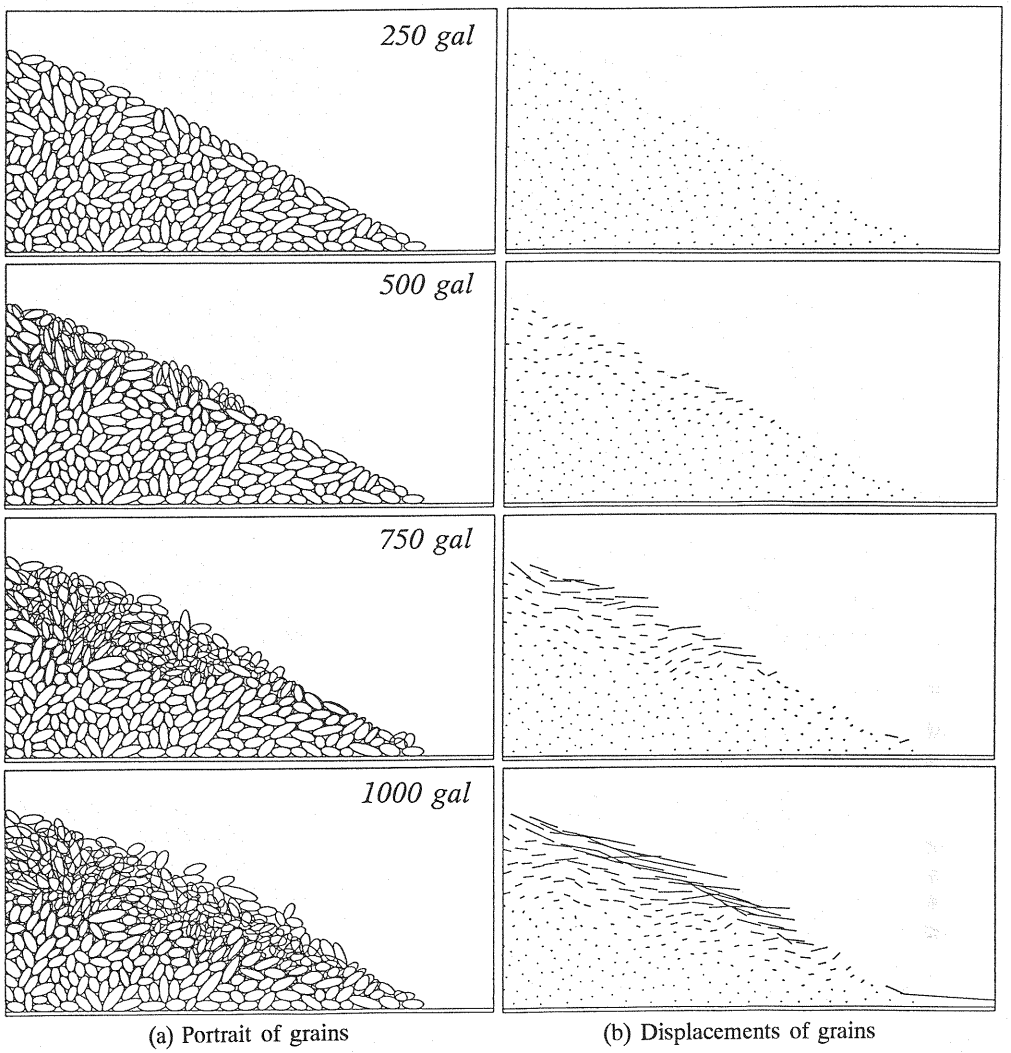

Fig. 12 Failure process of model A (500 ellipses)

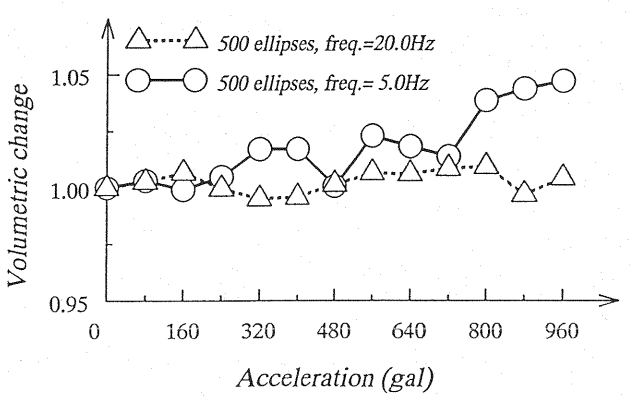

Fig. 13 Volumetric change of embankment (**model A**)

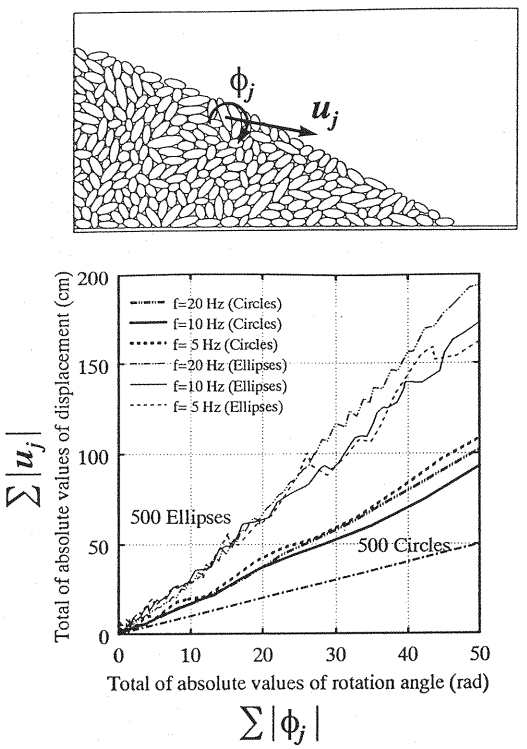

Fig. 14 Relation between overall displacement U_{ov} and rotation angle Φ_{ov}

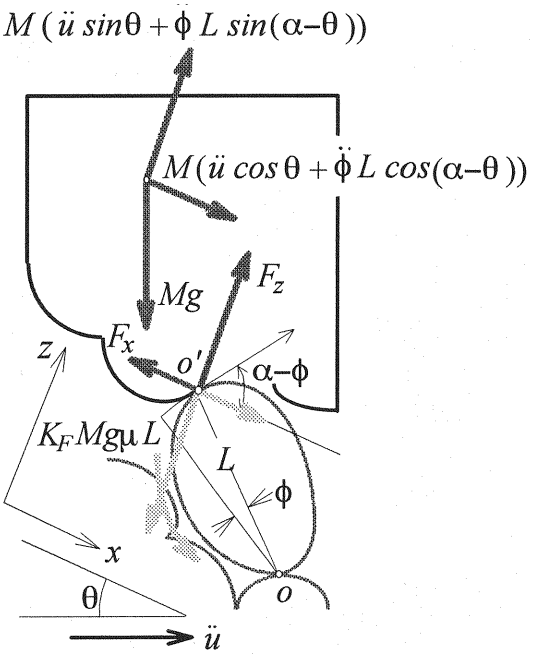

Fig. 15 Conceptual model of surface slide

4. CONCEPTUAL MODEL OF SLOPE FAILURE

Taking into account the considerable dilation observed in the course of the performed LAT experiments, a conceptual model of surface slide, shown in **Fig. 15**, is presented. In the model, one grain caught on a rough slip surface sustains a mass of surface grains, M. This mass moves downward after being once lifted on this grain, and the motion triggers the entire surface failure. During the process, the grain sustaining the mass may roll with its surface rubbing against the surrounding grains, or it may scarcely roll if it is embedded tightly. Either way, the bottom of the mass (point o') will orbit the point o through an angle ϕ being attended by an energy loss through friction, and consequently, the model is governed by the following equations as:

$$M(\ddot{u}\cos\theta + \ddot{\phi}L\cos(\alpha-\phi)) = Mg\sin\theta - F_x \quad \cdots(2)$$

$$M(\ddot{u}\sin\theta + \ddot{\phi}L\sin(\alpha-\phi)) = Mg\cos\theta - F_z \quad \cdots(3)$$

where, $\ddot{u}$ is an acceleration given to the model's base, and L is the radial distance from the center of rotation o to o', namely, the typical grain size. The initial gradient of upheaval of the grains' mass makes an angle, α, with the slip surface which dips by θ. The angle, α, therefore, may be equivalent to the so-called "angle of dilatancy", and shows how deeply grains engage with one another. Neglecting the inertia of the grain bearing the grains' mass, contact force components F_x and F_z should satisfy the following equilibrium of moment around point o:

$$F_x \cdot L\cos(\alpha-\phi) \cong F_z \cdot L\cos(\alpha-\phi) + K_F Mg\mu L \quad \cdots(4)$$

where, μ is a coefficient of friction between grains in contact, and K_F represents the contribution of inter-particle friction to the process of surface sliding, which may be hardly affected by the change in excitement frequency as shown in the previous DEM calculation. Assuming that the acceleration component in the direction normal to the slip surface (left-hand side of eq.(3)) is negligibly small, and that sines and tangents of angles α, θ and ϕ can be approximated by their angles α, θ and ϕ, respectively, eq. (2) can be rewritten as:

$$\ddot{\phi} - \frac{g}{L}\phi = \frac{g}{L}(\theta - \alpha - K_F\mu - \frac{\ddot{u}}{g}) = -\frac{g}{L}(\frac{\ddot{u}}{g} + \theta_0 - \theta) \quad \cdots(5)$$

If the inclination of the slope θ equals or exceeds $\alpha + K_F\mu$ in the above equation, no excitement is

needed to cause the surface mass to slip. In other words, $\alpha + K_F\mu$ here denotes the static angle of repose θ_0. Let the given acceleration $\ddot{u}$ be:

$$\ddot{u} = -a\sin(\omega t + \chi) \quad \cdots\cdots(6)$$

in which, χ is defined by the condition:

$$a\sin\chi = g\sin\alpha \quad \cdots\cdots(7)$$

This insures that the base acceleration reaches the value required to initiate motion of the mass at time t=0. Substituting eqs. (6) and (7) in eq. (3) results in:

$$\ddot{\phi} - \frac{g}{L}\phi = \frac{g}{L}(\theta_0 - \theta)\left(\frac{\sin(\omega t + \chi)}{\sin\chi} - 1\right) \quad \cdots\cdots(8)$$

This equation has the same form as that for a rocking rectangular block. Housner[7] solved it, and obtained a half-sine-wave acceleration pulse required for overturning a block. Picking up the procedures from Housner[7], a half-sine acceleration pulse required to initiate slip of the surface mass is obtained as:

$$a = g(\theta_0 - \theta)\sqrt{1 + \frac{L}{g}\omega^2} \quad \cdots\cdots(9)$$

This implies that the failure acceleration a is a function of only four parameters; critical angle of slope θ_0, slope inclination θ, representative grain size L and excitement circular frequency ω.

When an assemblage of particles is put within a liquid, buoyancy and drag[8] from the liquid should be taken into account. Their effect on the failure acceleration is easily incorporated only by replacing gravitational acceleration g with g' which is defined as:

$$g' = \frac{\gamma_g - \gamma_w}{\gamma_g + C_m\gamma_w}g \quad \cdots\cdots(10)$$

where, γ_g and γ_w are specific gravities of grain and liquid, respectively, and C_m is the added mass coefficient. The added mass coefficient should be determined by taking into account not only hydrodynamic pressure on the gently sloping surface of an embankment[8] but also grain-water-grain interaction. If the grain-water-grain interaction were negligibly small, many previous studies on drag force acting on a single grain would give us an idea how big the added mass coefficient is. Kotsubo and Takanishi[9], however, formulated disk-water-disk interaction, and showed that the added mass coefficient of a disk among the others is drastically changed if disks are closely spaced. It may be one extreme approximation to add pore water mass directly to the grains' mass because the water trapped within the pore of a grain assemblage will move with the grains if particles are densely packed. In this case, the added mass coefficient C_m will be about the same as the void ratio, e. The void ratio, e, varies in sand and gravel from 0.6 to 1.1, and consequently, the added mass coefficient C_m will lie within the same range. Whatever value the added mass coefficient takes, g' is always smaller than g, and the failure acceleration should be smaller than the one by eq. (9). Not only that, frequency dependence of failure acceleration should be clearer.

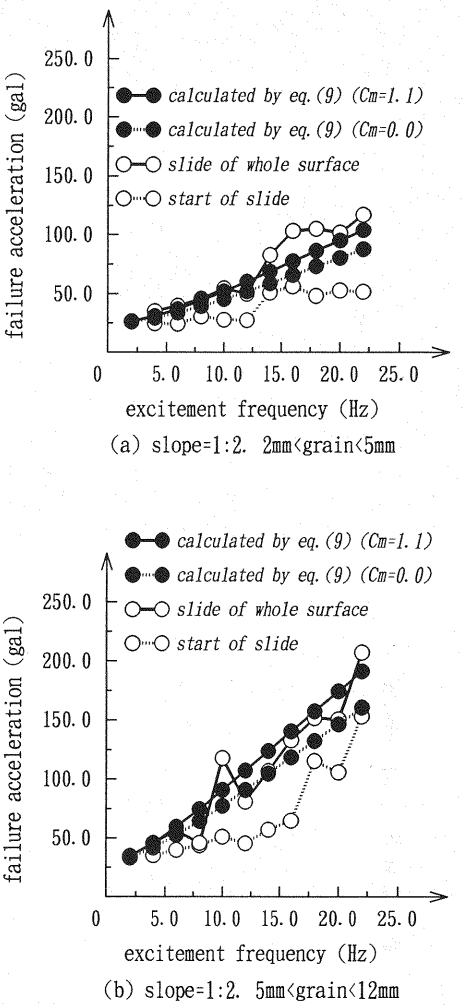

Fig. 16 Variation of failure acceleration with frequency

Figs. 16(a) and **16(b)** show the variations with excitement frequency of failure acceleration of the aforementioned two embankment models made up of smaller (2 mm < grain < 5 mm) and bigger (5 mm < grain < 12 mm) glass particles, respectively. In each figure, open circles connected by a broken line denote the accelerations required to initiate the surface slip (state like **Fig. 4(a)**), and those connected by a thick line show the accelerations at which the whole surface begins to slide (state like **Fig 4(b)**). On the other hand, solid circles show the failure accelerations calculated through eq. (9) assuming that the representative grain size L is the value in the middle of the grain size range.

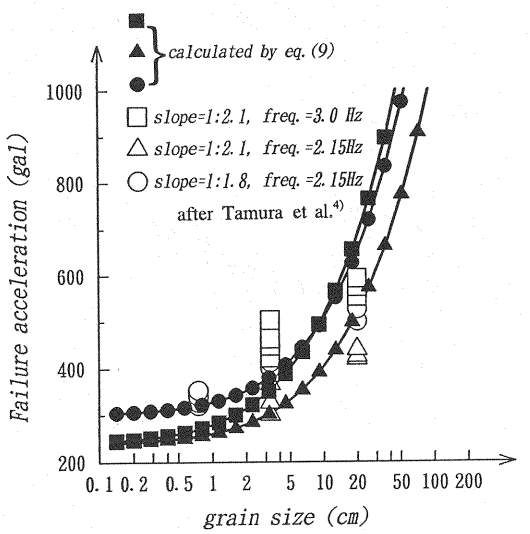

Fig. 16 Variation of failure acceleration with grain size

The value, $g'(\theta_0 - \theta)$ in eq.(9), showing static threshold was set at 25 gal for the finer grains' assemblage, and at 30 gal for the coarser grains. Since the biggest void ratio we can expect is about 1.1, the added mass coefficient C_m is expected to be smaller than this value. Thus, both extreme cases (C_m=1.1 and C_m=0.0) are shown in each figure. The result, however, is not sensitive to the change in C_m. The acceleration given to the embankment base was not a half-sine pulse used to obtain eq. (9) but a continuously increasing sine wave. And yet, the values calculated through eq. (9) (solid circles) will represent the threshold accelerations required to initiate the surface slip, because the observed surface failure was triggered off by a sudden and considerable dilation as shown in Fig. 5. Solid circles, however, seem to be plotted among the accelerations at which the failure spread over the entire surface (open circles connected by a thick line). It is noted here that the accelerations plotted were measured not on the slip surface, but on the model's base. This will be one of the reasons why the base acceleration required to initiate the surface failure is smaller than those by eq. (9).

Tamura, Okamoto and Kato[4] indicated through their experiments, that failure acceleration varies both with grain size and excitement frequency. They conducted dynamic failure tests on models of fill dams on a large-scaled shaking table (length = 10 m, width = 2 m, height = 4 m). The following five materials were used to make up the models; (1) sandy silt, (2)river-bed gravel (L=2~100 mm), (3)angular gravel (L=5~10 mm), (4)roundish gravel (L=20~600 mm) and (5)coarse marble (L=100~300 mm). **Fig. 17** shows variation of failure acceleration with grain size. Solid marks in this figure show calculated threshold acceleration using eq. (9) in which θ_0 is set at 43° picking up observed values in Ref. 4). As the acceleration becomes bigger, the observed threshold accelerations seem to become lower than the calculated values. Generally speaking, however, the bigger either the grain size or excitement frequency is, the bigger the threshold acceleration is, and this observed characteristic is also consistent with that of the conceptual model.

5. CONCLUSIONS

The failure process of a coarse particle assemblage is attended by a noticeable dilation which was observed through the new visualization technique, Laser-Aided Tomography (LAT). Numerical simulations by means of the discrete-elliptic-element method were conducted to study the failure process and frequency dependence of the failure acceleration, and a simple conceptual model of the surface failure was presented. Conclusions obtained through the study are summarized as follows:

(1) Prior to the calculation of the overall behavior, dynamic response of a single ellipse on a slope, to which a linearly increasing sinusoidal shake was given, was studied to clarify, in a simple manner, how the particle rolled or slid down at different frequencies. If the ellipse began to roll down, clear frequency dependence of the threshold acceleration appeared. The higher the excitement frequency was, the harder it rolled down because the rolling process is attended by a change in potential energy. On the contrary, when the ellipse slipped down, less dependence of the threshold acceleration appeared because this case is governed by Coulomb's hypothesis.

(2) Two embankment models made up of 500 ellipses (**model A**) and 500 circular disks (**model B**), respectively, were shaken in the same manner. Their dilation, as a whole, progressed slowly and steadily, and no sudden volumetric increase was clearly observed. Thus, it was not possible in this calculation to specify the threshold accelerations. In both cases, however, the lower the excitement frequency was, the more rapidly the failure progressed, and this phenomenon is consistent with the results from the LAT experiments.

(3) A change in the fabric of a granular assemblage is attended with both inter-particle slipping and grains' rolling. Contributions of these two key motions greatly affect the failure process. In the above calculation with 500 particles, it is noted that the contribution of both

inter-particle rolling and slipping to the failure process differs little at different excitement frequencies in both **model A** and **model B**. This implies that, given a specific material, the rolling-slipping ratio within the grain fabric during its failure process will be uniquely determined.

(4) Taking into account the considerable dilation observed in the course of LAT experiments, a conceptual model of surface slide was presented. In the model, a mass of particles moves downward after being once lifted on a rough slip surface. According to the proposed model, a half-sine acceleration pulse required to initiate surface failure is given as a simple function of only four parameters; static angle of repose θ_0, slope inclination θ, representative grain size L and excitement circular frequency ω. The variation of the failure acceleration either with grain size or with excitement frequency, observed through experiments, was consistent with the conceptual model, namely, the bigger either the grain size or excitement frequency is, the bigger the threshold acceleration is.

REFERENCES

1) Konagai, K. and C. Tamura: Visualization of Dynamic Change in Configuration of Underwater Particle Assemblage, Structural Dynamics, Kräzig et al. (eds.), Vol. 2, pp. 837-841, Balkema, Rotterdam, 1990.
2) Konagai, K., C. Tamura, P. Rangelow and T. Matsushima: Laser-Aided Tomography: A Tool for Visualization of Changes in the Fabric of Granular Assemblage, Structural Engineering / Earthquake Engineering, Vol. 9, No. 3, pp. 193s-201s, JSCE (Proc. of JSCE No. 455/I-21), 1992.
3) Hirata, K.: Fundamental Study on Dynamic Behavior of Embankment-shaped Granular Assemblage, Master Thesis, Univ. of Tokyo, 1990 (in Japanese).
4) Tamura, C., S. Okamoto and K. Kato: Dynamic Failure Tests on Rockfill Dam Models, "Tsuchi-to-Kiso", Japan Society of Soil Mechanics and Foundation Engineering, Vol. 20, No. 7, 1972 (in Japanese).
5) Matsushima, T. and K. Konagai: Failure Process of Coarse Particle Assemblage and its Frequency Dependency, Structural Dynamics - EURODYN'93, Moan et al. (eds.), Vol. 1, pp. 373-379, 1993.
6) Cundall, P.A.: A Computer Model for Simulating Progressive Large Scale Movement in Blocky Rock System, Symp. ISRM, Nancy, France, Proc., Vol. 2, pp. 129-136, 1971.
7) Housner, G.W.: The Behavior of Inverted Pendulum Structures During Earthquakes, Bull. of the Seismological Society of America, Vol. 53, No. 2, pp. 403-417, 1963.
8) Zanger, C.H.: Hydrodynamic Pressure on Dams due to Horizontal Earthquake Effects, U.S. Bureau of Reclamation, Engineering Monograph, No. 11, 1952.
9) Kotsubo, S. and T. Takanishi: A Method of Analysis of Dynamic Water Pressure during Earthquakes on Multi-Piles Foundation with Different Diameters and Arbitrary Position of Piles, Proc., JSCE, No. 276, pp. 1-12, 1978 (in Japanese).

(Received August 16, 1993)